Applied Energy 182 (2016) 219–231

Contents lists available at ScienceDirect

Applied Energy

journal homepage: www.elsevier.com/locate/apenergy

Influence of mill type on densified biomass comminution

Orla Williams [a,*], Gary Newbolt [a], Carol Eastwick [a], Sam Kingman [a], Donald Giddings [a], Stephen Lormor [b], Edward Lester [a]

[a] Faculty of Engineering, The University of Nottingham, University Park, Nottingham NG7 2RD, UK
[b] Engineering Team, EDF Energy plc., Cottam Power Station, Outgang Lane, Retford DN22 0EU, UK

HIGHLIGHTS

- Comminution of wide range of densified biomass in four mills.
- Shape factors do not change significantly compared to particle size with milling.
- Shape will only noticeably change below the critical particle size for comminution.
- Mill choking linked to the particle size, shape and classifier Stokes condition.
- Classification requirements should inform biomass pellet particle sizes.

ARTICLE INFO

Article history:
Received 13 April 2016
Received in revised form 17 August 2016
Accepted 18 August 2016
Available online 28 August 2016

Keywords:
Biomass
Stokes condition
Milling
Mill choking
Particle size
Particle shape

ABSTRACT

The impact of different mill fracture mechanisms were examined for a wide range of densified biomass pellets to provide a comprehensive analysis of biomass milling behaviour for pulverised fuel combustion. The milling behaviour of 7 woody, herbaceous, fruit, and thermally treated densified biomasses were investigated for four distinct types of comminution fracture mechanism using traditional milling indices and novel application of 3D imaging techniques. For the coal mill trials, a reference coal was used to provide a milling performance comparator. For the pre-milled samples, woody and herbaceous pellets have the least spherical particles (φ 0.324–0.404), followed by thermally treated pellets (φ 0.428), La Loma coal (φ 0.503), with olive cake having the most spherical particles (φ 0.562). This trend was noted for all the shape factors. Conventional comminution did not significantly impact biomass particle shape, even after a significant change in particle size. Therefore biomass pellet process history plays a key role in determining the comminuted particle shape. La Loma coal had significantly enhanced milling performance in comparison to the biomasses in the coal mills. Significant improvements in grindability and shape factors were observed for the thermally treated pellets. Mill choking was experienced for several of the woody and herbaceous samples, which resulted in a significant energy penalty. The mechanisms of mill choking were found to be intrinsically linked to the critical particle size of comminution through compression, particle shape factors, and the Stokes conditions set for the classifier and burners in pulverised fuel combustion systems. The study showed that for optimal milling performance, biomass pellets should be composed of particles which meet the Stokes requirements of the mill classifier. This would minimise the potential for mill choking and milling energy penalties, and ensure maximum mill throughput.

1. Introduction

Biomass is the biggest source of renewable energy in the EU and is expected to make a significant contribution to the 20% EU renewable energy target by 2020 [1]. Biomass conversion and co-combustion in coal fired power stations offers a low cost and high impact solution to reducing carbon emissions. However technical issues with using biomass in existing coal mills has led to mill blockages, fires, and reductions in boiler thermal output [2]. Biomass particle shape data is crucial in mill classifier and burner design and optimization [3], but there is only limited experimental data available in literature [4]. In this study, the impact of different mill fracture mechanisms on a wide range of different densified biomass pellets used for pulverised fuel combustion were examined in order to provide a comprehensive analysis of biomass milling behaviour.

* Corresponding author.
E-mail address: ezzow@nottingham.ac.uk (O. Williams).

http://dx.doi.org/10.1016/j.apenergy.2016.08.111
0306-2619/

Nomenclature

a	diameter of a circumscribed sphere around a particle (μm)
AR	particle aspect ratio (dimensionless)
C	circularity of a particle (dimensionless)
d	diameter of a sphere of the same volume as a particle (μm)
d'	Rosin-Rammler characteristic particle size (μm)
d_1	feed particle size (d_{80}) (μm)
d_2	product particle size (d_{80}) (μm)
d_{80}	particle size at 80th percentile of cumulative distribution (μm)
d_A	area equivalent diameter of a particle (μm)
d_P	perimeter equivalent diameter of a particle (μm)
d_{c_min}	shortest chord diameter (μm)
d_{Fe_max}	maximum Feret diameter (μm)
E_e	total effective specific energy (kW h/t)
HHV	higher heating value (J/g)
HHV_d	dry higher heating value (J/g)
K	Von Rittinger constant (dimensionless)
M	moisture content (%)
m	mass of sample in milling tests (g)
n	Rosin-Rammler size distribution parameter (dimensionless)
P	instantaneous power consumption (kW)
P_i	average idle power consumption (kW)
$R(d)$	Rosin-Rammler cumulative percentage undersize mass (%)
r_1 *and* r_2	distance from the centre of area of the borders in measuring direction (μm)
$Symm$	symmetry of a particle (dimensionless)
t	time (s)
φ	sphericity of a particle (dimensionless)

Legislation to reduce Nitrogen Oxide (NO_x) emissions in coal fired power stations has led to improvements in combustion efficiency through the introduction of low NO_x burners and improved fineness of coal particles [5]. The size of particles reaching the burner is dictated by the comminution equipment. Coal mills use static or dynamic pneumatic classifiers to select the correct cut size and consistency for combustion. For coal, the industry standard cut size for a classifier is that 75% of coal delivered to the burner must pass a 200 mesh screen (75 μm) [6], and for biomass the standard classifier setting is 1 mm [7]. Mill classifiers separate particles by using the Stokes condition based on the cut size [8]. The Stokes condition is a measure of the ability of particles to follow the surrounding flow [9], however it assumes spherical particles and thus shape factors need to be introduced for nonspherical particles. True sphericity was defined by Wadell [10] as the ratio of surface area of a sphere with the same volume as a particle to its actual surface area. As noted by Krumbein and Sloss [11], the measurement of true sphericity of an irregular particle is not feasible. Wadell [12] proposed a more practical definition of sphericity called Operational Sphericity (φ), which Krumbein and Sloss [11] defined as:

$$\varphi = \frac{d}{a} \tag{1}$$

where a is the diameter of a circumscribed sphere around a particle, and d is the diameter of a sphere of the same volume as the particle. As the Stokes condition is also dependent on a particle's Reynolds number; it is possible for large biomass particles to have similar aerodynamic properties to that of a much smaller coal particle provided they have a sufficiently low sphericity [13]. At present, solid fuel combustion prediction models rely on a spherical particle shape assumption [14], which may deviate from reality for large biomass particles [3]. Shape data is based on simplified shape assumptions of biomass shape, which is usually obtained from imaging [4]. Several studies have analysed the 2D shape factors of biomass through microscopy [15], 2D digital imaging [16–18], and 3D particle reconstruction algorithms have been developed to calculate sawdust particle surface area and volume [19]. However all these studies used small representative particle sizes, and there is no reported experimental data on the operational sphericity of comminuted biomass particles for large sample sizes.

In order to improve the bulk density for transportation, biomass is often milled to a coarse particle size then pelletized [20]. For the production of biomass pellets, feed stocks need to be comminuted so that at least 97% of the particles making up the pellet are below 3.35 mm in size [21]. Biomass milling studies have largely focused on non-densified woody, herbaceous, and agricultural residue biomasses in hammer and knife mills [7,18,22–37]. There are very few studies which consider the milling of densified biomass [38–41]. Planetary ball mills have been used to assess the improvement in grindability of torrefied biomasses through modified Hardgrove Grindability Index (HGI) tests [42,43], and used to develop hybrid work indices for torrefied materials [44]. There are limited accounts of biomass milling trials for coal mills in literature [41,45]. Studies tend to focus on standard coal grindability tests such as HGI [46,47] or Bond Work Index (BWI) test [39]. Very few studies compare the milling behaviour of different biomasses in different mills. Studies are generally limited to one biomass group such as woods in several types of mills [41], woods in a range of hammer mills [48], or herbaceous biomasses in a range of knife mills [31]. There are even fewer studies which look at the impact of milling on biomass shape factors. Torrefaction has been shown to improve biomass 2D shape factors [18], and reduce the agglomeration phenomenon characteristics of smaller particles of pulverised biomass, which leads to enhanced operation of pulverised biomass into boilers [49].

The aim of this study was to quantify the impact of different mill types commonly used in power generation on the milling behaviour and physical characteristics of several densified biomasses. This is the first study which investigates and compares the milling behaviour of woody, herbaceous, fruit, and thermally treated densified biomasses, along with a reference coal for the two coal mill tests, using four distinct types of comminution fracture mechanism. In addition, for the first time the impact of different milling operations on the operational sphericity of biomass particles has been assessed, and the paper demonstrates how this relates to the conditions used to select particles for combustion in full scale mills, particularly in relation to common mill operation issues such as mill choking, and the process history of the biomass pellets.

2. Materials and methods

2.1. Materials & pre-milling characterisation

The samples used (Fig. 1) are either routinely co-fired in coal fired power plants or have been used in biomass combustion trials. Portuguese mixed wood pellets (mainly pine (*Pinus*) with eucalyptus (*Eucalyptus grandis*)), Spanish olive cake (*Olea europaea*) - a residual waste mix from olive oil production, Russian sunflower

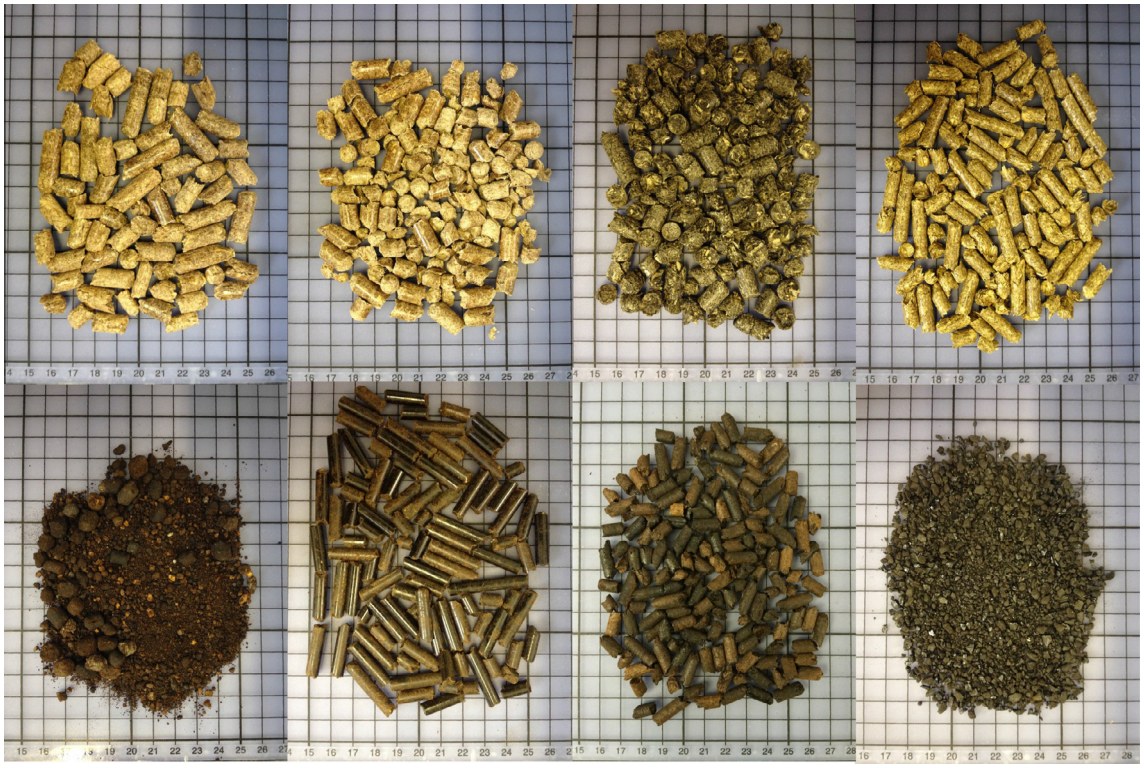

Fig. 1. (From top left to right) mixed wood pellets, eucalyptus pellets, sunflower husk pellets, miscanthus pellets, Spanish olive cake, steam exploded pellets, microwave pellets, La Loma coal. Scale is in cm grid.

husk (*Helianthus annus* L.) pellets; and Colombian La Loma coal were provided by EDF Energy plc. South African eucalyptus (*Eucalyptus grandis*) pellets, American steam exploded white wood chip pellets, and miscanthus (*Miscanthus* × *giganteus*) pellets were provided by E.ON UK plc. Steam exploded pellets are commercially produced by separating the lignin, cellulose and hemicelluloses components of woody biomass though both chemical degradation and mechanical deformation. The process involves adiabatic expansion of water inside the wood tissue pores and auto hydrolysis of cell components [50], and is known to improve pellet density, carbon content, and grindability [22,39,50,51]. Microwave torrefied white wood pellets, sourced from a commercial supplier, are produced by using microwave energy to directly and volumetrically heat woody biomass through pyrolysis at temperatures below 350 °C [52]. Microwave treatment improves pellet energy density and grindability, as well as creating a more hydrophobic material [35,53,54]. La Loma coal was included in the study to provide a reference coal against which the performance of the biomasses in coal mills could be compared. La Loma has a HGI value of 46, a standard HGI for coals burnt in UK coal fired power stations [39].

Moisture content was measured in accordance with BS EN 14774-1:2009 [55]. 300 g ± 1 g of each sample was dried in a Thermo Scientific Heraeus UT 6 forced-air oven at 105 °C ± 2 °C for 24 h. After drying the weight of the sample was recorded and used to calculate the moisture content of the biomass, with each sample being tested in triplicate. The Higher Heating Values (*HHV*) of the samples were found using an IKA C5000 Bomb Calorimeter in accordance with BS ISO 1928:2009 [56]. Certified Benzoic Acid tablets were used as a standard, and the sample weight was calibrated to give the same temperature rise as the standard. The test was conducted on as received samples, and thus the moisture content (M) as found above, was removed from the HHV values to give the dry HHV (HHV_d):

$$HHV_d = \frac{HHV}{1 - M} \tag{2}$$

The particle size range of the biomass particles (prior to densification) was obtained using the BS EN 16126:2012 [57]. 2 l of boiling deionised water was poured over 300 ± 1 g of each pellet sample and then soaked for 24 h. The samples were then dried at 35–60 °C until they reached 5–15% moisture content. The samples were then split into two portions; 150 g was used to obtain the moisture content via BS EN 14774-1:2009 [55], and the other 150 g was split and sieved according to BS 15149-2:2010 [58] to obtain a particle size distribution prior to comminution.

2.2. Comminution equipment

Four different mills were used as part of this study; a planetary ball mill, Bond ball mill, knife mill, and ring-roller mill. The mills are off-the-shelf unmodified laboratory mills, with the exception of the ring-roller mill, which is a bespoke one-off laboratory test mill. The planetary ball mill is a batch process without classification, the Bond ball mill uses the BWI methodology [59] to simulate a continuous milling operation by removing undersized milled product and replacing the equivalent mass with new material at calculated intervals until a steady state condition is achieved. The knife mill and ring-roller mill are continuous processes which use a screen and pneumatic classification respectively. Each mill uses a different fracture mechanism, as illustrated in Fig. 2. The planetary ball mill (Fig. 2A) uses high impact centrifugal compression fracture mechanisms by rotating the milling bowl and balls at high speeds, while the BWI mill (Fig. 2B) uses low impact compression fracture mechanisms by rotating the mill at low speeds and allowing gravity to cause a cateracting grinding ball motion. The knife mill (Fig. 2C) uses high shear forces to fracture and cut the material into smaller fragments through attrition, and the

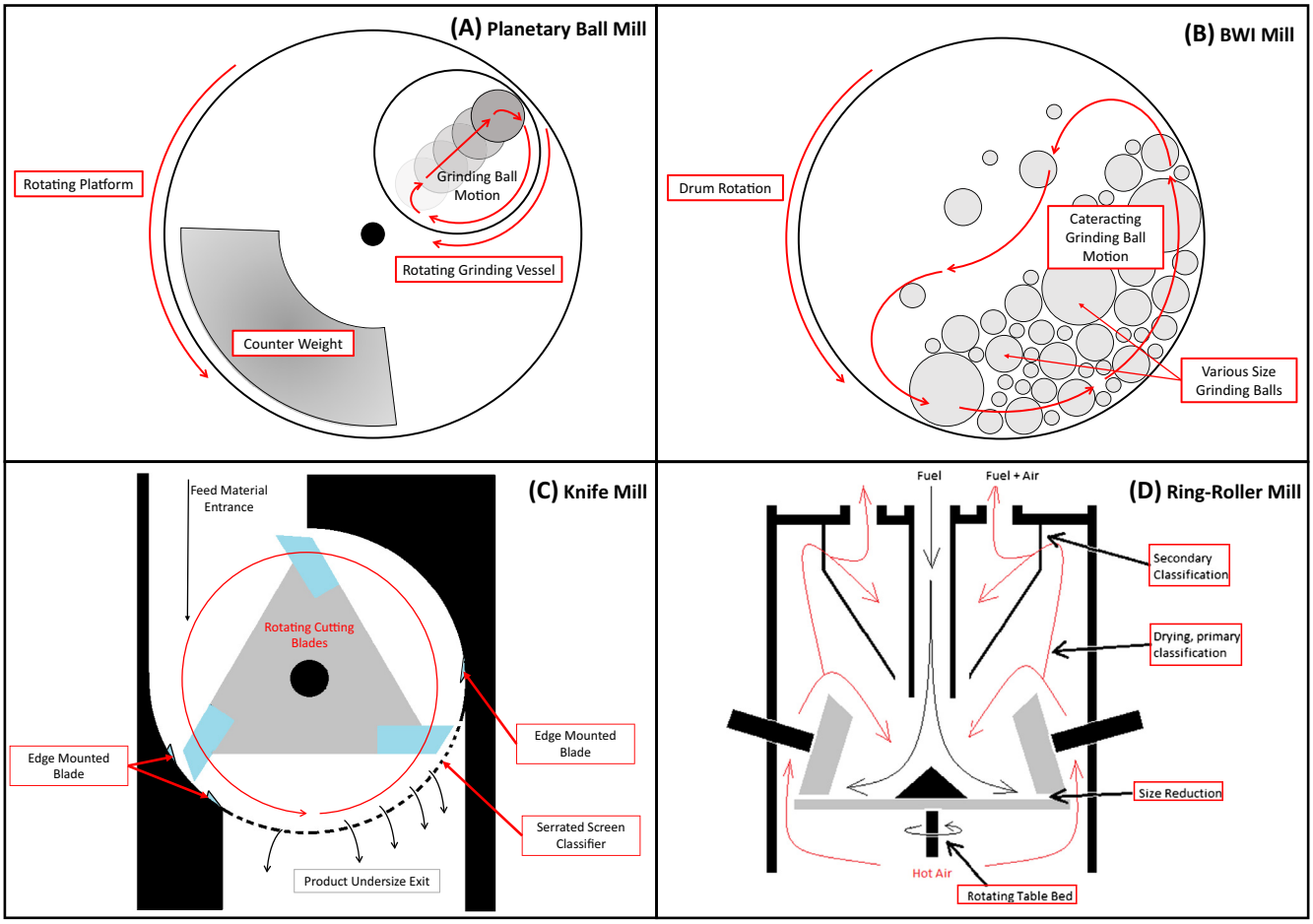

Fig. 2. Four different mills used for the milling trials; A – planetary ball mill, B – BWI mill, C – knife mill, D – ring-roller mill.

ring-roller (Fig. 2D) uses a mixture of compression and attrition fracture mechanisms as the material passes between the mill table and rollers. Constant volume was used instead of mass in the milling trials, as milling has been shown to be a volumetric process [42]; keeping the mass constant favours denser fuels with smaller specific volumes, and thus constant mass is unsatisfactory for making direct comparisons between fuels. Olive cake was not tested in the ring-roller mill as it formed a solid cake and became lodged within the mill, and tripped out the mill bed motors. La Loma coal was only tested in the two coal mill tests (Bond ball mill and ring-roller mill) due to limited sample availability.

Energy consumption was recorded using an Elcomponent SPC Pro for the knife mill and ring-roller mill. The total specific energy was calculated by integrating the Power-Time curve obtained from the data logger and then dividing by the material mass [40] to give the total energy consumed during the milling process (kW h/t). The total specific effective energy (E_e) was obtained by subtracting the specific idle energy from total specific energy for the run as measured by the energy logger [33,34]:

$$E_e = \int_0^t \frac{P dt}{m} - \int_0^t \frac{P_i dt}{m} \tag{3}$$

where P is the instantaneous power consumption (kW), P_i is the average idle power consumption (kW), t is time (h), and m is mass (tonne). Due to the varying classification settings of the mills, Von Rittinger's theory of comminution was used to compare the relationship between specific effective energy consumption and particle size reduction of the planetary ball mill, knife mill and ring-roller mill. The BWI energy consumption was not compared as the energy was estimated using Bond's third theory of comminution [59] rather than using an energy meter. Bond's theory is more applicable to this type of mill than Von Rittinger's theory of comminution. The BWI test is a proven application for sizing tube-ball mills and is a true grindability parameter [60]. Von Rittinger's first theory of comminution states that "*The energy required for size reduction is proportional to the new surface area generated*" [61], and is expressed as:

$$E_e = K\left(\frac{1}{d_2} - \frac{1}{d_1}\right) \tag{4}$$

where K is the constant characteristic for the material, d_1 is the 80th feed passing size (μm), and d_2 is the 80th product passing size (μm).

2.2.1. Planetary ball mill

A standard Retsch PM100 planetary ball mill was used for the planetary ball milling trials with a 500 ml stainless steel milling bowl and eight 30 mm diameter stainless steel balls. The PM100 planetary ball mill has a 0.75 kW drive unit, and total power draw of 1.25 kW. 100 ml of each sample was milled for 3 min at a milling speed of 300 RPM. The input energy consumed was measured directly by the planetary ball mill [62] and the specific effective energy consumption was found by dividing this energy input by the mass of the sample. All milling trials were repeated in triplicate.

2.2.2. Bond Ball Mill

A standard Bico Ball Mill was used to conduct the standard BWI test on a range of biomasses and sample coal [59]. The mill

contains 285 steel balls of total weight 20.13 kg with a drum size of 305 mm in diameter by 305 mm in length which rotates at a constant speed of 70 RPM. The details of the test can be found in a previous study [39]. The closing sieve size selected was 1 mm for biomass and 75 μm for coal. All milling trials were repeated in duplicate.

2.2.3. Knife mill

A standard Retsch SM300 knife mill was used for the knife mill trials. The SM300 knife mill has a 3 kW drive with additional auxiliary flywheel mass and speed range of 700–3000 RPM. A 4 mm sieve was used at a speed of 1500 RPM and the sample was continuously fed into the mill via a vibrating bed feeder at an average feed rate of 20 kg/h. 400 ml of sample was used for each run and all milling trials were repeated in triplicate.

2.2.4. Ring-roller mill

The Lopulco LM 1.6 is a laboratory scale continuous throughput ring-roller mill which has not previously been reported in biomass milling literature. The mill is a bespoke one-off experimental test mill and is around 40 years old, but was fully refurbished before this study. The system has a 2.2 kW fan, 0.65 kW mill bed motor, 0.37 kW feeder motor and 0.12 kW rotary valve motor. In the system the air is recirculated in a closed loop system, with air being fed to the underside of the mill and then pulled through to the cyclone where the particles drop out and the air returns to the fan. Material is placed in a hopper which feeds directly into a variable speed screw feeder. The feed flows directly into the mill which has variable speed rotating table and two rollers supported by adjustable hinged spring lever arms that rest clear of the table, setting the roll gap. The material is pushed under the rollers by oncoming feed and the spinning table. The separator is connected to the mill table via a vertical shaft. Milled material flows to the outer rim of the table, is lifted pneumatically by the air entering through the base of the milling chamber, and carried up to the top of the milling chamber, exiting through the separator. If the material is sufficiently fine it will pass through the separator while the oversize material is returned to the mill for further comminution. The milled product, which is classified by the separator, flows pneumatically to a cyclone where the material is separated from the air stream. The material from the cyclone falls into a surge bin that feeds a constant speed rotary air lock which maintains system pressure and allows the cyclone to continuously remove material from the air stream. 1 kg of densified biomass was tested in triplicate, and 600 g of La Loma coal was tested in duplicated tests due to limited supplies. The mill bed was set to a speed of 200 RPM, and the screw feeder was set to run at 70 RPM, resulting in a mass feed rate of approximately 7 g/s for the biomass pellets and 10 g/s for the coal due to the density variations of the fuels.

2.3. Particle size distribution by sieving

Particle size distributions were determined by sieving the milled product in accordance with BS EN 15149-2:2010 [58]. The samples were sieved into 16 size fractions; 4750, 3350, 2360, 1700, 1180, 1000, 850, 600, 425, 300, 212, 150, 75, 53, 45, 38 μm sieves. Sieving was conducted on a Retsch AS200 control vibratory sieve shaker in two stages. In the first stage, 8 coarse sized sieves (4750–600 μm) were used, and in the second stage, 8 finer sieves (450–38 μm) were used. Each sieving stage was conducted for 15 min at 3 mm amplitude.

2.4. Particle size characterisation

The Rosin-Rammler distribution equation was originally developed to describe the distribution of coal fines from coal mills [63], and it has been shown that the Rosin-Rammler distribution equation is a good fit for biomass comminution in hammer mills [29,33]. The Rosin-Rammler equation is:

$$R(d) = 100\left(1 - e^{-(d/d')^n}\right) \tag{5}$$

where R is cumulative percentage undersize mass (%), d is particle diameter (μm), d' is the characteristic particle size (μm), defined as the size at which 63.2% ($1 - 1/e = 0.632$) of the particles (by weight) are smaller, and n is the Rosin-Rammler size distribution parameter (dimensionless). The Rosin-Rammler parameters were found using the Matlab® GUI Tool developed by Brezáni and Zelenak [64]. The particle size distributions of percentage retained mass against particle size were plotted on semi-logarithmic plots.

2.5. Particle shape distributions

Particle shape analysis was conducted on a Retsch Camsizer® P4. The Retsch Camsizer P4 measuring system is based on 3D digital imaging processing [65]. The sample was split using a riffle box 6 times prior to measurement to ensure that a representative portion of the sample was analysed. The particles flow along a vibratory bed feeder until they drop into a slot and pass between a light source and two high speed cameras. The particles were individually detected as projected areas, digitalised and the images processed. The measurements were analysed in the Retsch Particle Library software (version 1.4.1) in wizard mode [66]. By screening the results for the 50th percentile of the shape cumulative distribution (Q_{50}), a particle list was created for the filtered sizes (particles within the range of the set value +0.001), and representative images were selected. The sample size was approximately 2–5 million particles depending on the fineness of the sample.

2.6. Particle shape characterisation

The results of the particle shape characteristics are based on the shortest chord diameter ($d_{c\_\min}$) [67]. The shortest chord diameter ($d_{c\_\min}$) can be considered as equivalent to the particle size achieved from sieving. The aspect ratio (AR) is the ratio of the width of a particle to its length, which in the case of the measured parameters is equivalent to the ratio of the shortest chord diameter to the maximum Feret diameter ($d_{FE\_\max}$), which is the longest distance between two parallel tangents of the particle at any arbitrary angle [67]:

$$AR = \frac{d_{c\_\min}}{d_{Fe\_\max}} \tag{6}$$

The measured sphericity is the operational sphericity as defined by Krumbein and Sloss [11], as defined in Eq. (1), and has a value between 0 and 1, with 1 being a perfect sphere. Circularity (C) is a measure of how closely a particle resembles a circle, considering the smoothness of the perimeter and is determined in accordance with BS ISO 9276-6 [68], and is a measure of the roundness of a particle [69].

$$C = \frac{d_A}{d_P} \tag{7}$$

where d_A is the area equivalent diameter of the particle and d_P is the perimeter equivalent diameter of the particle. The Camsizer software squares the circularity to give a value between 0 and 1, with an ideal circle having a value of 1 [67]. The Symmetry ($Symm$) of particles indicates the level of symmetry in the particles of a given size class, and is defined as [67]:

$$Symm = \frac{1}{2}\left(1 + min\left(\frac{r_1}{r_2}\right)\right) \tag{8}$$

where r_1 and r_2 are distances from the centre of area to the borders in the measuring direction. For asymmetric particles *Symm* is < 1. If the centre of area is outside the particle i.e. $r_1/r_2 < 0$, then *Symm* < 0.5. The symmetry is a minimum value of a measured set of symmetry values from different directions.

3. Results & discussion

The results of the milling trials provide a comprehensive overview and novel insight into the diverse range of milling behaviours of different densified biomasses. Due to extensive nature of the results presented, they are categorised firstly by material group, followed by commonalities and variances in milling behaviour, the mechanisms of mill choking, and the implications of the results on future milling research and full scale milling operations. The milling results are summarised in Figs. 3 and 4, with additional data in Table 1. Fig. 3 shows specific effective energy consumption for the planetary ball mill, BWI mill, knife mill, and ring-roller mill by biomass type.

The most notable overall result is the incredibly high milling energy for the BWI test, which is detailed in a previous publication by the authors [39]. This is due to mill choking. Mill choking is the phenomenon by which the rate of feeding into a mill is faster than the rate at which it can be evacuated from the mill. For full scale coal mills with classifiers and recycle, mill choking happens when the mill is unable to reduce the particles to a size and shape suitable for meeting the Stokes conditions of the classification system. Further feeding into the mill results in increased circuit load due to the necessity of the still oversized material to be recycled and subjected to further comminution. The higher load increases the requirement for energy due to an elongated residence time for comminution. The mechanisms behind this phenomenon and the impact on milling behaviour are discussed later in this paper. Table 1 comprehensively characterises the samples prior to milling and for each milling process. It contains particle size characterisation through the Rosin-Rammler analysis of the particle size distributions, the relationship between specific effective energy and particle size through the Von Rittinger constant, and impact of milling on the shape properties of the particles. Fig. 4 illustrates the impact of milling on the sphericity of the particles through the milling process. Through these results, the influence of process history and material properties can be elicited on the milling behaviour, providing novel insight into the comminution of biomass for power generation applications.

3.1. Woody biomass

The mixed wood and eucalyptus pellets fall within the woody category of biomass according to BS EN 172251 [70]. The wood pellets had some of the highest energy consumptions of all the samples. Mixed wood pellets choked in the ring-roller and BWI mills (Fig. 3), and had the highest energy consumption in the knife mill (32.5 ± 0.5 kW h/t). In contrast, eucalyptus pellets were on the lower end of energy consumption for the non-treated biomasses (87 ± 8.7 kW h/t), with a similar energy consumption to the steam exploded pellets in the BWI test (64 ± 0.8 kW h/t). Comminution in all mills had a similar impact on particle size for both woods, with eucalyptus producing a finer particle size distribution than the mixed wood for lower energy consumptions (Fig. 3 and Table 1). For eucalyptus pellets, the planetary ball mill produced the finest distribution (d′ 493 μm) followed by the BWI (d′ 541 μm), while the opposite trend was observed for mixed wood pellets (d′ 628 μm for planetary ball mill, d′ 530 μm for BWI). The knife and ring-roller mills show little impact on the pre-milled particle sizes. For the knife mill, this was related to the selected screen size for the knife mill (4 mm) and thus the pellets broke down into their pre-milled size and passed through the screen. The ring-roller used pneumatic classification which was set to allow maximum throughput, which allowed for coarse particles to pass the aerodynamic barrier. Eucalyptus particles saw little change in sphericity through milling despite a significant change in particle size in the planetary ball mill and BWI mill. The mixed wood particles saw an increase in sphericity in all the mills (Fig. 4), demonstrating significant variances in milling behaviour within the same biomass group. When the energy consumption is also taken into account (Fig. 3), eucalyptus pellets show a greater change in particle size for a much lower energy consumption in all mills compared to the mixed wood pellets. Thus eucalyptus particles reduce more easily in size with little change in shape for less milling effort than the mixed wood particles.

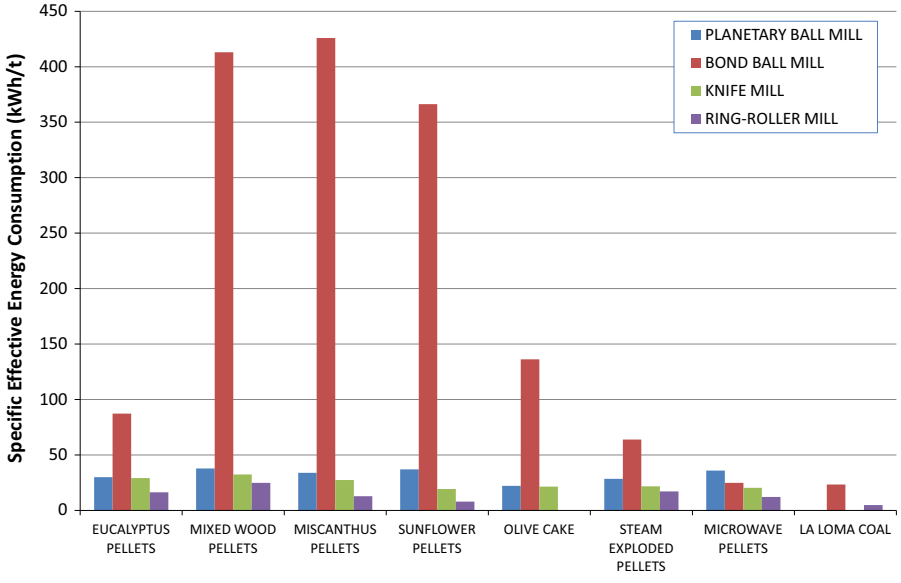

Fig. 3. Specific effective energy consumption for different mills by biomass and coal type.

Sphericity Q_{50}	Pre-milled	Planetary Ball Mill	Bond Work Index	Knife Mill	Ring-Roller Mill
Eucalyptus Pellets	 0.404	 0.398	 0.409	 0.409	 0.382
Mixed Wood Pellets	 0.347	 0.381	 0.387	 0.384	 0.403
Miscanthus Pellets	 0.324	 0.330	 0.339	 0.355	 0.343
Sunflower Pellets	 0.347	 0.384	 0.418	 0.397	 0.382
Olive Cake	 0.562	 0.577	 0.490	 0.535	
Steam Exploded Pellets	 0.428	 0.454	 0.455	 0.464	 0.445
Microwave Pellets		 0.464	 0.385	 0.414	 0.403
La Loma Coal	 0.503		 0.506		 0.403

Fig. 4. Particle shape outline for 50th percentile of sphericity φ for all samples in all mills. N.B. olive cake was not milled in the ring-roller mill, microwave pellets did not disintegrate in the disintegration test, and La Loma coal was not milled in the planetary ball mill or knife mill.

3.2. Herbaceous biomass

Sunflower and miscanthus pellets fall into the herbaceous biomass group according to BS EN 17225-1 [70]. The particle size reduction of the herbaceous samples were not dissimilar to the woody pellets. In spite of having some of the highest energy consumptions, there was little impact on the particle size in the planetary ball mill, knife mill, and ring-roller mill (Table 1). The only real difference was observed in the BWI test where both the sunflower (d_{80} 757 μm) and miscanthus (d_{80} 813 μm) pellets choked, resulting in the very high specific effective energy consumption (Fig. 3). It is notable that in the ring-roller mill test, where neither sample choked, sunflower had the lowest energy consumption of all the densified biomasses (7.9 ± 1.3 kW h/t). Sunflower pellets biggest increase in sphericity was observed in the BWI test (0.375–0.426), which also resulted in its largest reduction in particle size. The high energy consumption for the BWI test (366 ± 0.5 kW h/t) shows that a large effort was involved in achieving this change in particle size and shape. For the other shape factors, sunflower and miscanthus particles saw a decrease in

Table 1
Pre-milled and milled 80th percentile particle size (d_{80}), Von Rittinger constant (K) Rosin-Rammler analysis, mean sphericity (φ), mean circularity (C), mean aspect ratio (AR), and mean symmetry (Symm).

Sample/mill	d_{80} (μm)	Von Rittinger constant (K)	Rosin-Rammler analysis			Mean φ	Mean C	Mean AR	Mean $Symm$
			d' (μm)	n	R^2				
Eucalyptus pellets (HHV_d 20,348 J/g)									
Pre-milled	1215	–	833	1.40	1.000	0.432	0.545	0.544	0.745
Planetary ball mill	705	17.9	493	1.27	1.000	0.428	0.504	0.539	0.742
Bond ball mill	751	–	541	1.62	0.997	0.440	0.487	0.548	0.702
Knife mill	1171	0.9	901	1.69	1.000	0.441	0.543	0.553	0.772
Ring-roller mill	958	3.6	721	1.63	1.000	0.414	0.504	0.524	0.751
Mixed Wood Pellets (HHV_d 20,652 J/g)									
Pre-milled	1373	–	966	1.29	0.998	0.376	0.492	0.484	0.781
Planetary ball mill	975	11.3	628	1.15	0.999	0.409	0.439	0.519	0.743
Bond ball mill	787	–	530	1.28	0.989	0.414	0.422	0.524	0.736
Knife mill	1105	5.7	847	1.72	0.999	0.413	0.494	0.526	0.765
Ring-roller mill	1201	2.6	814	1.36	0.998	0.429	0.490	0.540	0.696
Miscanthus pellets (HHV_d 18,669 J/g)									
Pre-milled	1251	–	832	1.38	0.992	0.353	0.508	0.455	0.795
Planetary ball mill	1181	1.6	898	1.32	0.999	0.356	0.461	0.461	0.747
Bond ball mill	813	–	582	1.64	0.994	0.366	0.431	0.470	0.728
Knife mill	1069	3.7	1038	1.47	0.999	0.384	0.486	0.492	0.754
Ring-roller mill	1377	-0.9	1035	1.64	0.998	0.375	0.457	0.480	0.735
Sunflower pellets (HHV_d 20,755 J/g)									
Pre-milled	1744	–	1115	1.18	0.995	0.375	0.567	0.481	0.797
Planetary ball mill	1220	9.1	822	1.24	0.999	0.412	0.499	0.521	0.742
Bond ball mill	757	–	557	1.82	0.997	0.452	0.495	0.559	0.670
Knife mill	1145	5.9	763	1.70	1.000	0.426	0.525	0.539	0.771
Ring-roller mill	1523	0.7	1089	1.09	0.999	0.413	0.500	0.525	0.763
Olive cake (HHV_d 20,264 J/g)									
Pre-milled	3360	–	1953	0.93	0.997	0.584	0.757	0.692	0.863
Planetary ball mill	1553	8.2	925	1.09	0.998	0.592	0.741	0.698	0.853
Bond ball mill	589	–	360	1.22	0.997	0.520	0.625	0.637	0.802
Knife mill	1461	10.1	1122	1.55	0.999	0.560	0.742	0.673	0.851
Steam exploded pellets (HHV_d 20,397 J/g)									
Pre-milled	1196	–	889	1.35	0.998	0.458	0.620	0.577	0.816
Planetary ball mill	466	37.3	310	1.14	0.998	0.484	0.518	0.602	0.760
Bond ball mill	346	–	201	0.97	0.999	0.484	0.511	0.601	0.749
Knife mill	1412	-2.8	1038	1.75	1.000	0.498	0.648	0.615	0.821
Ring-roller mill	521	18.6	394	1.61	0.999	0.477	0.609	0.594	0.795
Microwave pellets (HHV_d 21,261 J/g)									
Planetary ball mill	285	–	185	1.13	0.999	0.480	0.577	0.597	0.769
Bond ball mill	888	–	668	1.96	0.992	0.414	0.590	0.528	0.805
Knife mill	1091	–	859	1.80	1.000	0.445	0.629	0.561	0.813
Ring-roller mill	538	–	417	1.76	1.000	0.435	0.577	0.551	0.786
La Loma coal (HHV_d 29,665 J/g)									
Pre-milled	2723	–	1954	1.46	0.992	0.532	0.710	0.645	0.836
Bond ball mill	78	–	59	2.81	0.983	0.536	0.605	0.651	0.771
Ring-roller mill	402	10.2	281	1.29	0.999	0.543	0.617	0.650	0.758

symmetry and circularity, and increase in aspect ratio with milling, which is the same trend as seen for the mixed wood pellets (Fig. 4).

3.3. Fruit biomass

Olive cake is a fruit biomass according to BS EN 17225-1 [70]. Olive cake had some of the lowest energy consumptions of the non-treated biomasses (Fig. 3). The olive cake was the only non-treated biomass to show a significantly different milling output in all the mills. Olive cake produced the finest non-treated biomass particle size distribution in the BWI test (d' 360 μm), but much coarser product in the planetary ball mill (d' 925 μm) and knife mill (d' 1122 μm). Due to its composition, olive cake also produced the most spherical particles after milling. Wood is a low density, cellular polymeric composite of hemicellulose, cellulose, and lignin (HCl), and all biomasses are composed of varying quantities of HCl [71]. The needle like structure which is visible in particle outlines of the wood and herbaceous particles (Fig. 4) is due to this composite structure [71]. Olive cake on the other hand is made of two components [72]; a stone where the lignin is concentrated, and the outer pulp or flesh where the hemicellulose and cellulose is concentrated, resulting in rounder and more spherical particles (Table 1 and Fig. 4). The olive cake saw a notable change in sphericity in the BWI mill (11% decrease), but this was accompanied by its largest change in particle size. This trend was also true for the symmetry, aspect ratio and circularity, which also saw little change through milling apart from in the BWI mill.

3.4. Thermally treated biomass

The steam exploded and microwave pellets fall into the thermally treated biomass group, and show the most dissimilar results to any other group. The microwave pellets proved to be hydrophobic during the pellet disintegration test, and retained their original size and shape with no swelling. This implies that the microwave thermal treatment has resulted in a fundamental change in the structure of the material. Unlike the other pellets, the microwave pellets are composed of material which has been permanently

fused together by the microwave process. Unfortunately no data on the pre-densified particle size distributions was available for the microwaved pellets. The thermally treated pellets showed the lowest energy consumptions of all the biomasses (Fig. 3). While the energy consumption was generally similar for the two thermally treated pellets, the microwave pellets energy consumption was over half that of the steam exploded pellets in the BWI test (Fig. 3). The thermally treated biomasses show very different particle size distributions and particle shape factors compared to the woody pellets (Table 1 and Fig. 4). There was a significant reduction in particle size for different mills compared to the woody biomasses, highlighting that thermal treatment does significantly improve the grindability of woody biomasses. This has been noted in several previous studies for non-densified biomasses [18,22,35–37,39,42,44,46,47], but has not previously been shown for steam exploded and microwave thermally treated biomass pellets. Microwave and steam exploded pellets had noticeably improved all shape factors compared to the woody biomasses. Thus thermal pre-treatment also improves the shape factors of the particles, as previously noted for non-densified biomass [18]. This shows that thermal pre-treatments are creating biomass particles which are more spherical and closer to those of coal particles, which will allow for better mixing and particle flow in pulverised fuel systems.

3.5. Coal

La Loma coal was tested in the ring-roller and BWI mill to provide a benchmark against which the performance of the biomasses could be compared. It had the lowest energy consumption (4.8 ± 2.7 kW h/t) and smallest particle size in the ring-roller mill (d' 281 μm), and achieved similar energy consumption to the microwave pellets for a much finer particle target size in the BWI test (23 ± 0.1 kW h/t). Only the thermally treated pellets had comparable energy consumptions (Fig. 3), but for a much larger product particle size. There was little change in the particles shape factors despite a significant change in particle size for the La Loma coal (Table 1 and Fig. 4); which signifies that the brittle fracture mechanisms of coal result in considerably more efficient comminution than can be achieved for biomass. The La Loma coal results demonstrate that comminuting biomass in a coal mill will result in a significant loss in performance, and thus with lower mill throughputs. With the added penalty of reduced higher heating values (Table 1), biomass combustion in coal fired power stations will inevitably lead to reduced mill throughput and thermal output and a reduction in potential power generation.

3.6. Commonalities and variances in densified biomass comminution

Each of the mills in this study used a different fracture mechanism for particle size reduction (Fig. 2), and also had distinct classification systems. Apart from the BWI mill, most mills show similar specific effective energy consumptions (Fig. 3); the ring-roller mill has the lowest energy consumptions (4.8 ± 2.7–24.9 ± 7 kW h/t), followed by the knife mill (19.3 ± 2.4–32.5 ± 0.5 kW h/t) and finally the planetary ball mill (22.2 ± 1.4–37.9 ± 1.7 kW h/t). These specific energy values are similar to those summarised by Temmerman et al. [38] for non-densified and densified woody biomasses in hammer and knife mills. However, despite similar energy consumptions being recorded for all mills apart from the BWI mill, very different product sizes were obtained (Table 1). By comparing the Von Rittinger constant (K) for these three mills (Table 1), it is clear than some mills have achieved a greater particle size reduction for a similar specific effective energy consumption. In general, the planetary ball mill showed the highest K values, followed by the ring-roller mill and knife mill. However the results are material dependent. The woody pellets showed the highest K values in the planetary ball mill (17.9 for mixed wood and 11.3 for eucalyptus). The miscanthus pellets showed very low K values in all mills (−0.9 in the ring-roller mill to 3.7 in the knife mill), indicating that none of the mills significantly reduced its particle size. The steam exploded pellets showed very high K values in the planetary ball mill (37.3), but negative values in the knife mill (−2.8), as the mill broke the pellets into chunks rather than particles. The results suggest that the most effective fracture mechanism is material dependent. This is linked to the target size of the mill and the ability of the material to reach that size.

The dry higher heating value (HHV_d) of the materials ranged between 18,669 J/g and 21,261 J/g for biomass and 29,665 J/g for coal (Table 2). The specific effective energy consumption generally represented a small amount of HHV_d. The planetary ball mill saw the lowest percentage for olive cake (0.39%) and highest for mixed wood (0.66%). Sunflower showed the lowest (0.33%) percentage, with mixed wood the highest (0.57%), for the knife mill. For the ring-roller mill, La Loma showed the lowest (0.06%) whilst mixed wood showed the highest (0.43%). The BWI test showed significantly higher percentages for the materials which choked, with miscanthus (8.21%), mixed wood (7.20%) and sunflower (6.35%), which is an order of magnitude higher than La Loma (0.28%) and Microwave pellets (0.42%). This highlights the impact mill choking has not just on mill performance, but on how thermal output is compromised by non-optimal milling conditions; this would result in a significant loss of output for a power generator.

The particle shape factors provide novel insights into the milling behaviour of biomass and coal. Fig. 5 shows the cumulative distribution of particle sphericity of the samples prior to testing. The cumulative distributions are based on the sphericity of particles as a percentage of tested sample volume. For the pre-milled samples, woody and herbaceous pellets have the least spherical particles, followed by the thermally treated pellets, La Loma coal, with olive cake having the most spherical particles. This trend was noted for all the shape factors (Fig. 4 and Table 1). Comminution did not significantly change the particle shape factors, even when a significant change in particle size was observed. For La Loma coal, an order of magnitude of particle size change was observed between the pre-milled and milled particle sizes, but resulted in little change in particle shape. There were also significant reductions in particle size for olive cake, steam exploded pellets and microwave treated pellets in the mills, but once more their sphericity showed little change. Thus the pre-milled particle shape of biomass and coal is inherent in informing the particle shape

Table 2
Percentage milling energy represents of the samples dry higher heating values (HHV_d).

Sample (HHV_d)	Planetary ball mill	Bond mill	Knife mill	Ring-roller mill
Eucalyptus pellets (20,349 J/g)	0.53	1.54	0.52	0.29
Mixed wood pellets (20,652 J/g)	0.66	7.20	0.57	0.43
Miscanthus pellets (18,669 J/g)	0.65	8.21	0.53	0.25
Sunflower pellets (20,755 J/g)	0.64	6.35	0.33	0.14
Olive cake (20,264 J/g)	0.39	2.42	0.38	–
Steam exploded pellets (20,397 J/g)	0.50	1.13	0.38	0.30
Microwave pellets (21,261 J/g)	0.61	0.42	0.34	0.20
La Loma coal (29,665 J/g)	–	0.28	–	0.06

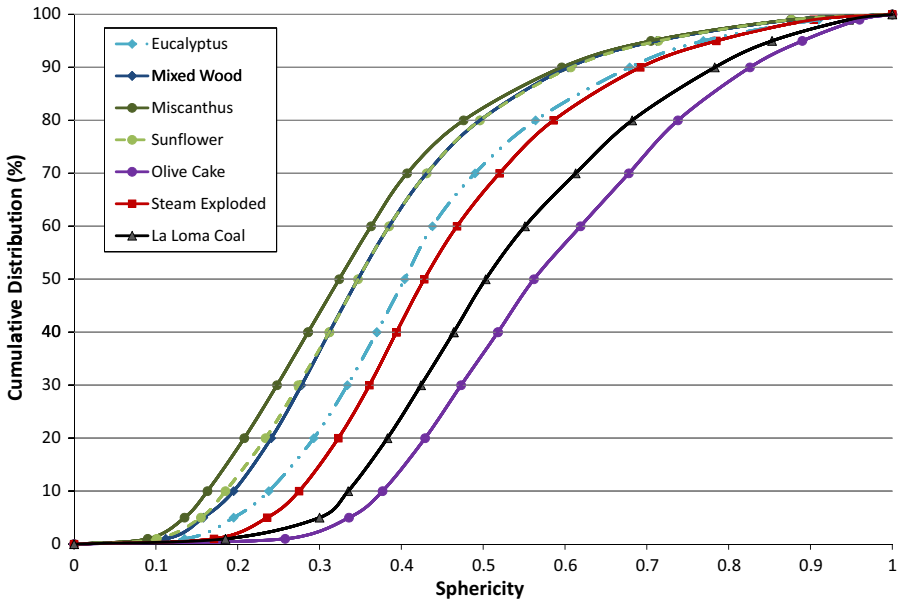

Fig. 5. Cumulative distribution of particle sphericity for the pre-milled samples.

after milling, even if there is an order of magnitude change in the particle size.

3.7. Mechanisms of mill choking

The BWI test observed significantly higher specific effective energy consumption for several of the samples (mixed wood pellets 413 ± 3.7 kW h/t, miscanthus pellets 425.9 ± 29.5 kW h/t, sunflower pellets 366.3 ± 0.5 kW h/t), which was due to these samples choking in the mill. As noted in a previous paper by the authors [39], the pre-densified particle size of the pellets was a key feature in mill choking in the BWI mill. In a batch operation such as the BWI test, which aims to simulate continuous milling, mill choking means that the mill never reaches a steady state condition of milling. For the BWI test, the revolution count never stabilised and the grindability per revolution stabilised to a very low value. In the ring-roller mill, steady state was also not achieved for the mixed wood pellets. The mass output flowrate (4.1 g/s) was less than two thirds of its feed mass flowrate (7.0 g/s) for the mixed wood pellets, while the other biomasses input and output mass flow rates were almost equal, indicating steady state operation. When mill choking was observed, a greater change in shape factors was observed for a small change in particle size due to attrition (Fig. 4). The mixed wood pellets showed a small change in particle size (pre-milled d_{80} 1373 μm, milled d_{80} 1201 μm) in the ring-roller mill for the highest specific energy consumption. However there was a 14% increase in average sphericity for this relatively small reduction in particle size, the largest change in shape for any of the materials.

The mechanisms of mill choking can be linked to the fracture mechanisms used in the mills and the material fracturing properties. Coal is a brittle material and fractures originate from stress-activated flaws, and in practice different particle sizes break at different rates [73]. Smaller coal particles require higher energy inputs to break, as there is less chance of finding a large flaw in a smaller volume of a small particle. Thus the repeated use of size reduction will result in stronger smaller solid particles, and eventually the energy required to initiate failure will be larger than that which can be achieved. This is the point at which the critical particle size for comminution through compression is reached [74], beyond this the material behaves as if it is ductile under compression and size reduction will only be possible through attrition. This length is material dependant and it is known to be around 5 μm for coal, however the values for biomass are unknown. The results of this study suggests that below the critical particle size for comminution through compression, the shape of the particle will only start to change by attrition, the only remaining mechanism of size reduction available; this results in a slower comminution process than size reduction through compression, and hence mill choking occurs.

In contrast to coal, biomass does not have an inherent crack system. Wood is an orthotropic material and has two or three mutually orthogonal twofold axes of rotational symmetry, resulting in anisotropic mechanical properties [71]. In wood, cracks will generally grow along the wood fibres, irrespective of both the original notch orientation and the mode of fracture [75]. Cracks oriented parallel to the wood fibres grow self-similarly, while cracks originally oriented across the wood fibres hardly ever grow in their own plane; instead they make a perpendicular kink and extend along the fibres immediately after onset of fracture, giving wood particles their needle like shape. The fibre-composite structure of wood means that it deforms elastically, however its brittle behaviour is dominated by tension perpendicular to the grain and shear, while compression failure parallel to the grain is ductile in nature, with plastic deformation before failure. Due to this complex combination of failure mechanisms and the varying composition of biomass, the critical particle size for comminution will vary between biomass types.

The results of this study indicate that the planetary bill mill can give an indicative value for the critical particle size of comminution for biomass. When the d_{80} particle size of the planetary ball mill was smaller than the d_{80} of the BWI test, no choking was observed. However, if the opposite was true, choking was observed. The d_{80} particle size for the microwave pellets in the BWI test (888 μm) was significantly above that obtained in the planetary ball mill (285 μm), while the steam exploded pellets obtained a finer d_{80} in the BWI test (346 μm) than in the planetary ball mill (466 μm). The steam exploded pellets' energy consumption was nearly 3 times that of the microwave pellets in the BWI mill, but similar to the microwave pellets for all the other mills when the

milled product was coarser than that obtained in the planetary ball mill. This trend was noted for all biomasses which choked in the BWI test. This indicates that the planetary ball mill is reducing the material to a particle size close to its critical particle size for comminution through compression [74].

3.8. Implications for biomass milling research and industry

This study has several major implications for future milling research and biomass comminution in full scale mills. The study has shown that there will be little change in a biomass particle's shape unless it chokes within the mill. As conventional milling leads to no significant change in the particle shape factors, the process history of the biomass is fundamental in influencing the comminuted particle shape; this will play a leading role in determining its ability to pass an aerodynamic barrier. The other key parameter is the materials critical particle size of comminution for which, where biomasses are concerned, there is no data currently, and research is required in this area in order to gain greater insight into biomass milling. Thus, for biomasses to be used in pulverised fuel combustion systems knowledge of these two parameters is fundamental for optimal milling and combustion. The comparison to La Loma coal milling performance highlights that when the milling of biomass particles is required, there will be a significant reduction in milling performance. To mitigate this, pellets should be composed of particles of the correct size and shape to pass through the classifier, and thus milling will only need to break down the weak pellet bonds. This would eliminate the issue of mill choking, minimise the milling energy penalty, and ensure maximum mill throughput. Beyond this, the pre-densified particle shape factors can be used in turn to inform CFD models, which can then inform classifier set up and pellet specifications. This would allow for CFD combustion models to be more closely linked to experimental milling and combustion research.

The correlation between particle size and shape in laboratory scale milling trials is of paramount importance in understanding its applicability to full scale systems. Fig. 6 shows the relationship between particle shape and size for the four mills. The correlations noted are indicative of the behavioural trends of the mill classification systems. No correlation was observed for the planetary ball mill, which is to be expected as no classification system is used. The knife mill showed a linear relationship, with increasing particle size resulting in increasing sphericity, which does not fit the Stokes equation relationship. The knife mill used a 4 mm screen which resulted in the pellets only breaking down into their pre-densified sizes (Table 1). The knife mill uses a screen rather than the Stokes condition to select particles, which is similar to full scale hammer mills. However at UK power stations such as EDF Cottam, the hammer mills are used as part of a semi-direct injection system feeding pulverised fuel burners. The product from the hammer mills is injected into the pneumatic flow from the tube-ball mills and delivered to the burners as a mix of coal and biomass. Therefore even though the hammer mill is not using the Stokes condition to select the particle size, the screen selection should be such that the comminuted particles have the correct physical parameters for optimal pneumatic flow and for complete combustion. The ring-roller mill tests show that classification results in a wide spread of particle sizes due to the varying density and sphericity of the different materials. Both the BWI and ring-roller mills showed increasing sphericity with decreasing particle size, which fits the Stokes requirements. The ring-roller mill highlights how pneumatic classification will result in varying product sizes for different biomasses. Current biomass milling research is focused on grinding tests rather than grinding and classification. This study has shown that for biomass milling studies, classification cut size based on burner requirements should be used to determine the target size of laboratory milling trials.

4. Conclusion

This paper provides a comprehensive overview of the milling behaviour of a wide range of densified biomasses in different mills. The comminution of densified biomass is intrinsically linked to the raw material composition, comminution behaviour, and milled product characteristics. The pre-densified particle size and pre-densified particle shape are determined by the process history of densified biomass; these two key factors will control the comminution behaviour. This study uniquely observed that comminution does not significantly impact biomass particle shape even when there is a significant change in particle size, and thus the process history of biomass pellets determines the comminuted particle shape. For the pre-milled samples, woody and herbaceous

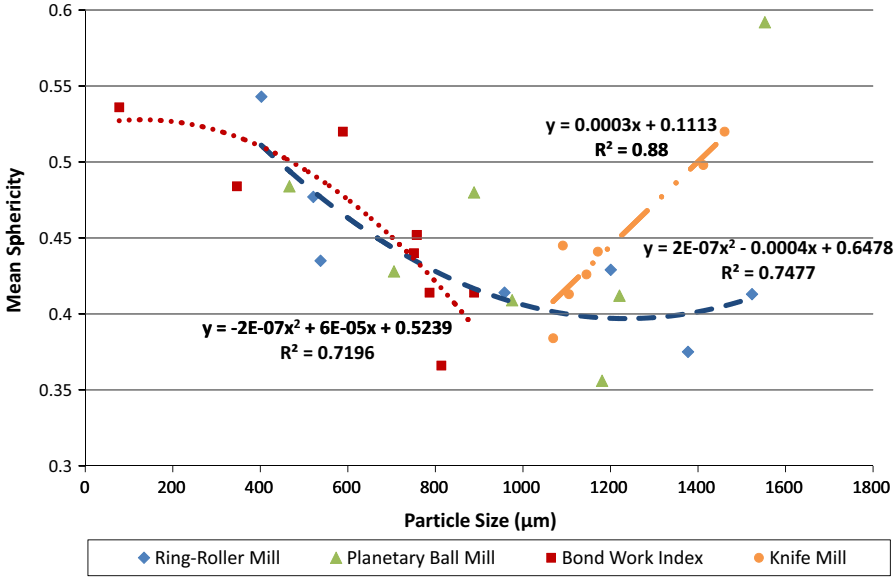

Fig. 6. Mean sphericity and particle size (d_{80}) for different biomasses and coals comminuted in different mills.

pellets have the least spherical particles (φ 0.324–0.404), followed by the thermally treated pellets (φ 0.428), La Loma coal (φ 0.503), with olive cake having the most spherical particles (φ 0.562).

The study indicated that the most effective fracture mechanism is dependent upon the material, and is linked to the target size of the mill, as well as the ability of the material to reach that size. La Loma coal had significantly enhanced milling performance in the ring-roller and BWI mills due to the favourable fracture mechanisms employed in these mills for brittle materials. In order to compensate for this when using biomass pellets, care should be taken to ensure that the pellets are composed of particles of the correct size and shape to pass through the classifier. Comminution would therefore only need application to breaking down the weak bonds formed during the pellet making process. The consequences of this would be maximising mill throughput and increasing the energy potential of the fuels.

A common operational issue experienced with densified biomass is mill choking. This study identified that the mechanisms of mill choking are intrinsically linked to the critical particle size of comminution through compression, particle shape factors, and the Stokes conditions set for a pulverised fuel combustion system's classifier and burners. Particles will not significantly change shape until this critical particle size is met, after which the only mode of size reduction available is through attrition, leading to slower comminution, and induced mill choking. As a consequence, steady state milling cannot be achieved, resulting in poor milling performance and a significant energy penalty on the fuel; for an energy generator this results in a loss of potential power generation. Currently no data exists on the critical particle size for comminution of biomass. Further research is required to determine this for commonly used biomasses and the impact this has on the milling of densified biomass in relation to their process history.

Acknowledgements

This research is funded and supported by the Biomass & Fossil Fuel Research Alliance (BF2RA), EDF Energy plc, and the Engineering and Physical Sciences Research Council (EPSRC) [Grant number EP/G037345/1]. The study was part of an Engineering Doctorate at the Efficient Fossil Energy Technology Centre in the Faculty of Engineering at The University of Nottingham. The authors would like to thank all those involved for their support and cooperation during the course of the research.

References

[1] European Commission. State of play on the sustainability of solid and gaseous biomass used for electricity, heating and cooling in the EU [SWD (2014)259] 2014.
[2] Savolainen K. Co-firing of biomass in coal-fired utility boilers. Appl Energy 2003;74:369–81.
[3] Tabet F, Gökalp I. Review on CFD based models for co-firing coal and biomass. Renew Sustain Energy Rev 2015;51:1101–14.
[4] Rosendahl LA, Yin C, Kær SK, Friborg K, Overgaard P. Physical characterization of biomass fuels prepared for suspension firing in utility boilers for CFD modelling. Biomass Bioenergy 2007;31:318–25.
[5] Larsen KJ. Pulverised biomass and coal co-firing simulation using computational fluid dynamics PhD thesis. The University of Leeds; 2012.
[6] Afolabi JL. The performance of a static coal classifier and its controlling parameters PhD thesis. University of Leicester; 2012.
[7] Esteban LS, Carrasco JE. Evaluation of different strategies for pulverization of forest biomasses. Powder Technol 2006;166:139–51.
[8] Fuerstenau MC. Principles of mineral processing. Society for Mining, Metallurgy and Exploration, Inc. (SME); 2003.
[9] Toneva P, Wirth KE, Peukert W. Grinding in an air classifier mill - Part II: Characterisation of the two-phase flow. Powder Technol 2011;211:28–37.
[10] Wadell H. Volume, shape, and roundness of rock particles. J Geol 1932;40:443–51.
[11] Krumbein WC, Sloss LL. Properties of sedimentary rocks. In: Gilluly J, Woodford AO, editors. Stratigr Sediment. W.H. Freeman and Company; 1963. p. 106–13.
[12] Wadell H. Volume, shape and roundness of quartz particles. J Geol 1935;43:250–80.
[13] Mandø M, Rosendahl L, Yin C, Sørensen H. Pulverized straw combustion in a low-NOx multifuel burner: modeling the transition from coal to straw. Fuel 2010;89:3051–62.
[14] Holtmeyer ML, Kumfer BM, Axelbaum RL. Effects of biomass particle size during cofiring under air-fired and oxyfuel conditions. Appl Energy 2012;93:606–13.
[15] Guo Q, Chen X, Liu H. Experimental research on shape and size distribution of biomass particle. Fuel 2012;94:551–5.
[16] Cardoso CR, Oliveira TJP, Santana Junior JA, Ataíde CH. Physical characterization of sweet sorghum bagasse, tobacco residue, soy hull and fiber sorghum bagasse particles: density, particle size and shape distributions. Powder Technol 2013;245:105–14.
[17] Gil M, Teruel E, Arauzo I. Analysis of standard sieving method for milled biomass through image processing. Effects of particle shape and size for poplar and corn stover. Fuel 2014;116:328–40.
[18] Phanphanich M, Mani S. Impact of torrefaction on the grindability and fuel characteristics of forest biomass. Bioresour Technol 2011;102:1246–53.
[19] Lu H, Ip E, Scott J, Foster P, Vickers M, Baxter LL. Effects of particle shape and size on devolatilization of biomass particle. Fuel 2010;89:1156–68.
[20] Obernberger I, Thek G. Pellet production and logistics. Pellet Handb. First, Earthscan Ltd.; 2010, p. 85–129.
[21] The British Standards Institution. BS EN ISO 17225-2:2014 - Solid biofuels — Fuel specifications and classes. Part 2: Graded wood pellets; 2014: 20.
[22] Adapa P, Tabil LG, Schoenau G. Grinding performance and physical properties of non-treated and steam exploded barley, canola, oat and wheat straw. Biomass Bioenergy 2011;35:549–61.
[23] Bitra V, Womac AR, Yang YT, Igathinathane C, Miu PI, Chevanan N, et al. Knife mill operating factors effect on switchgrass particle size distributions. Bioresour Technol 2009;100:5176–88.
[24] Bitra V, Womac AR, Yang YT, Miu PI, Igathinathane C, Sokhansanj S. Mathematical model parameters for describing the particle size spectra of knife-milled corn stover. Biosyst Eng 2009;104:369–83.
[25] Chevanan N, Womac AR, Bitra V, Igathinathane C, Yang YT, Petre IM, et al. Bulk density and compaction behaviour of knife mill chopped switchgrass, wheat straw, and corn stover. Bioresour Technol 2010;101:207–14.
[26] Mani S, Tabil LG, Sokhansanj S. Grinding performance and physical properties of wheat and barley straws, corn stover, and switchgrass. Biomass Bioenergy 2004;27:339–52.
[27] Gil M, Luciano E, Arauzo I. Population balance model for biomass milling. Powder Technol 2015;276:34–44.
[28] Gil M, Arauzo I. Hammer mill operating and biomass physical conditions effects on particle size distribution of solid pulverized biofuels. Fuel Process Technol 2014;127:80–7.
[29] Gil M, Arauzo I, Teruel E, Bartolomé C. Milling and handling *Cynara Cardunculus* L. for use as solid biofuel: experimental tests. Biomass Bioenergy 2012;41:145–56.
[30] Gil M, Arauzo I, Teruel E. Influence of input biomass conditions and operational parameters on comminution of short-rotation forestry poplar and corn stover using neural networks. Energy Fuels 2013;27:2649–59.
[31] Miao Z, Grift TE, Hansen AC, Ting KC. Energy requirement for comminution of biomass in relation to particle physical properties. Ind Crops Prod 2011;33:504–13.
[32] Laskowski J, Lysiak G. Use of compression behaviour of legume seeds in view of impact grinding prediction. Powder Technol 1999;105:83–8.
[33] Bitra VS, Womac AR, Chevanan N, Miu PI, Igathinathane C, Sokhansanj S, et al. Direct mechanical energy measures of hammer mill comminution of switchgrass, wheat straw, and corn stover and analysis of their particle size distributions. Powder Technol 2009;193:32–45.
[34] Himmel H, Tucker M, Baker J, Rivard C, Oh K, Grohmann K. Comminution of biomass: hammer and knife mills. In: Proc. 7th symp biotechnol fuels chem, Gatlinburg, Tennessee, 14–17 May, 1985. John Wiley; 1986. p. 39–58.
[35] Satpathy SK, Tabil LG, Meda V, Naik SN, Prasad R. Torrefaction of wheat and barley straw after microwave heating. Fuel 2014;124:269–78.
[36] Arias B, Pevida C, Fermoso J, Plaza MG, Rubiera F, Pis JJ. Influence of torrefaction on the grindability and reactivity of woody biomass. Fuel Process Technol 2008;89:169–75.
[37] Repellin V, Govin A, Rolland M, Guyonnet R. Energy requirement for fine grinding of torrefied wood. Biomass Bioenergy 2010;34:923–30.
[38] Temmerman M, Jensen PD, Hébert J. Von Rittinger theory adapted to wood chip and pellet milling, in a laboratory scale hammermill. Biomass Bioenergy 2013;56:70–81.
[39] Williams O, Eastwick C, Kingman S, Giddings D, Lormor S, Lester E. Investigation into the applicability of Bond Work Index (BWI) and Hardgrove Grindability Index (HGI) tests for several biomasses compared to Colombian La Loma coal. Fuel 2015;158:379–87.
[40] Gravelsins RJ, Trass O. Analysis of grinding of pelletized wood waste with the Szego Mill. Powder Technol 2013;245:189–98.
[41] Tamura M, Watanabe S, Kotake N, Hasegawa M. Grinding and combustion characteristics of woody biomass for co-firing with coal in pulverised coal boilers. Fuel 2014;134:544–53.
[42] Bridgeman TG, Jones JM, Williams A, Waldron DJ. An investigation of the grindability of two torrefied energy crops. Fuel 2010;89:3911–8.
[43] Ibrahim RHH, Darvell LI, Jones JM, Williams A. Physicochemical characterisation of torrefied biomass. J Anal Appl Pyrol 2013;103:21–30.

[44] Van Essendelft DT, Zhou X, Kang BS-J. Grindability determination of torrefied biomass materials using the hybrid work index. Fuel 2013;105:103–11.
[45] Zulfiquar MH, Wall TF, Moghtaderi B. Co-milling of coal and biomass in a pilot-scale vertical spindle mill. QCAT Technol Transf Cent; 2006.
[46] Shang L, Ahrenfeldt J, Holm JK, Sanadi AR, Barsberg S, Thomsen T, et al. Changes of chemical and mechanical behavior of torrefied wheat straw. Biomass Bioenergy 2012;40:63–70.
[47] Ohliger A, Förster M, Kneer R. Torrefaction of beechwood: a parametric study including heat of reaction and grindability. Fuel 2013;104:607–13.
[48] Paulrud S, Mattsson JE, Nilsson C. Particle and handling characteristics of wood fuel powder: effects of different mills. Fuel Process Technol 2002;76:23–39.
[49] Chen WH, Cheng WY, Lu KM, Huang YP. An evaluation on improvement of pulverized biomass property for solid fuel through torrefaction. Appl Energy 2011;88:3636–44.
[50] Biswas AK, Yang W, Blasiak W. Steam pretreatment of Salix to upgrade biomass fuel for wood pellet production. Fuel Process Technol 2011;92:1711–7.
[51] Adapa P, Tabil LG, Schoenau G. Physical and frictional properties of non-treated and steam exploded barley, canola oat and wheat straw grinds. Powder Technol 2010;201:230–41.
[52] Rotawave Ltd. The case for energy densification of biomass & the advantage of the rotawave ties system - executive summary 2010:4. <http://www.canadian-biocoal.com/articles/Rotawave>. TIES system advantage Jun 2010_final_pdf [accessed July 1, 2016].
[53] Lanigan BA. Microwave processing of lignocellulosic biomass for production of fuels PhD thesis. University of York; 2010.
[54] Robinson J, Kingman S, Baranco R, Snape CE, Al-Sayegh H. Microwave pyrolysis of wood pellets. Ind Eng Chem Res 2010;49:459–63.
[55] The British Standards Institution. BS EN 14774-1:2009 - Solid biofuels. Determination of moisture content. Oven dry method. Total moisture. Reference method; 2009: 12.
[56] The British Standards Institution. BS ISO 1928:2009 Solid mineral fuels — Determination of gross calorific value by the bomb calorimetric method and calculation of net calorific value; 2009.
[57] The British Standards Institution. BS EN 16126:2012 — Solid biofuels. Determination of particle size distribution of disintegrated pellets; 2012: 16.
[58] The British Standards Institution. BS EN 15149–2:2010: Solid biofuels. Determination of particle size distribution. Vibrating screen method using sieve apertures of 3,15 mm and below; 2010: 18.
[59] Bond FC. Crushing and grinding calculations. Br Chem Eng 1961;6:378–85.
[60] Csöke B, Bokányi L, Bohm J, Pethö S. Selective grindability of lignites and their application for producing an advanced fuel. Appl Energy 2003;74:359–68.
[61] von Rittinger PR. Lehrbuch der Aufbereitungskunde. Berlin: Ernst and Korn; 1867.
[62] Retsch Gmbh. Operating Instructions Ball Mills; 2012. <http://www.retsch.com/dltmp/www/53e4b55a-36f8-4c5a-9812-636500000000-c58b206a07da/manual_pm100_pm200_pm100cm_en.pdf>.
[63] Rosin P, Rammler E. The laws governing the fineness of powdered coal. Inst Fuel 1933;7:29–36.
[64] Brezáni I, Zelenak F. Improving the effectivity of work with Rosin-Rammler diagram by using MATLAB®GUI tool. Acta Montan Slovaca 2010;15:152–7.
[65] Allen T. Powder sampling and particle size determination. Elsevier; 2003.
[66] Retsch Gmbh. Installation & Operation Manual - PARTICLE LIBRARY: WIZARD MODE 2015:1–54.
[67] Retsch Gmbh. CAMSIZER® Characteristics 2009: 8. <http://www.horiba.com/fileadmin/uploads/Scientific/Documents/PSA/Manuals/CAMSIZER_Characteristics_Nov2009.pdf>.
[68] The British Standards Institution. BS ISO 9276-6:2008 - Representation of results of particle size analysis. Descriptive and quantitative representation of particle shape and morphology; 2008: 34.
[69] Wadell H. The coefficient of resistance as a function of Reynolds number for solids of various shapes. J Franklin Inst 1934;217:459–90.
[70] The British Standards Institution. BS EN ISO 17225-1:2014 Solid biofuels. Fuel specifications and classes. General requirements; 2014: 68.
[71] Dinwoodie JM. Timber: its nature and behaviour. Routledge; 2000.
[72] Kailis S, Harris DJ. Producing table olives. Australia: Landlinks Press; 2007.
[73] Klimpel RR. Fine coal grinding. In: Klimpel RR, Klimpel RR, editors. Fine coal process. Noyes Publications; 1987. p. 19–58.
[74] Kendall K. The impossibility of comminuting small particles by compression. Nature 1978;272:710–1.
[75] Jernkvist LO. Fracture of wood under mixed mode loading I. Derivation of fracture criteria. Eng Fract Mech 2001;68:549–63.